Edward A. Sander[1]
Department of Biomedical Engineering,
University of Iowa,
Iowa City, IA 52242;
Department of Surgery,
University of Cincinnati College of Medicine,
Cincinnati, OH 45267;
Research Department
Shriners Hospital for Children, Cincinnati,
Cincinnati, OH 45267
e-mail: edward-sander@uiowa.edu

Kaari A. Lynch
Department of Surgery
University of Cincinnati College of Medicine
Cincinnati, OH 45267;
Research Department
Shriners Hospital for Children, Cincinnati,
Cincinnati, OH 45267

Steven T. Boyce
Department of Surgery,
University of Cincinnati College of Medicine
Cincinnati, OH 45267;
Research Department
Shriners Hospital for Children, Cincinnati,
Cincinnati, OH 45267

Development of the Mechanical Properties of Engineered Skin Substitutes After Grafting to Full-Thickness Wounds

Engineered skin substitutes (ESSs) have been reported to close full-thickness burn wounds but are subject to loss from mechanical shear due to their deficiencies in tensile strength and elasticity. Hypothetically, if the mechanical properties of ESS matched those of native skin, losses due to shear or fracture could be reduced. To consider modifications of the composition of ESS to improve homology with native skin, biomechanical analyses of the current composition of ESS were performed. ESSs consist of a degradable biopolymer scaffold of type I collagen and chondroitin-sulfate (CGS) that is populated sequentially with cultured human dermal fibroblasts (hF) and epidermal keratinocytes (hK). In the current study, the hydrated biopolymer scaffold (CGS), the scaffold populated with hF dermal skin substitute (DSS), or the complete ESS were evaluated mechanically for linear stiffness (N/mm), ultimate tensile load at failure (N), maximum extension at failure (mm), and energy absorbed up to the point of failure (N-mm). These biomechanical end points were also used to evaluate ESS at six weeks after grafting to full-thickness skin wounds in athymic mice and compared to murine autograft or excised murine skin. The data showed statistically significant differences ($p < 0.05$) between ESS in vitro and after grafting for all four structural properties. Grafted ESS differed statistically from murine autograft with respect to maximum extension at failure, and from intact murine skin with respect to linear stiffness and maximum extension. These results demonstrate rapid changes in mechanical properties of ESS after grafting that are comparable to murine autograft. These values provide instruction for improvement of the biomechanical properties of ESS in vitro that may reduce clinical morbidity from graft loss.
[DOI: 10.1115/1.4026290]

Introduction

Permanent wound closure is critical to the survival of patients with massive burns, traumatic injuries, or congenital conditions that require the replacement of significant portions of their skin [1,2]. It is estimated that as many as 500,000 burns are treated in the U.S. every year with approximately 20,000 of these resulting in hospitalization [3]. Advances in burn care have significantly reduced mortality rates for massive burns. From 2003–2012, pediatric burn injuries covering 50% of their total body surface area (TBSA) or greater had an average of 29.4% mortality [3]. These survival rates are achieved by providing a regimen of critical care that is costly and requires lengthy hospitalizations. Furthermore, in those instances where TBSA is high and donor sites for skin autograft are not readily available, the need for an alternative skin substitute may become definitive.

Several tissue-engineering strategies have been developed to improve permanent wound closure for patients with massive burns or other injuries that require the replacement of significant portions of their skin [1,4,5]. These strategies generally involve the use of degradable polymer scaffolds, cells, or some combination of the two and have provided significant benefits to patients by providing a life-saving barrier that promotes rapid healing and stable wound closure [6,7]. However, many skin substitutes suffer from poor mechanical properties and can be easily damaged during handling or by tensile or shear forces in situ after transplantation. Even after remodeling and integrating with the host tissue, the repaired tissue often does not recover the mechanical properties of native skin and the extracellular matrix (ECM) is never restored to its uninjured condition [8–10].

Previous studies from this laboratory have reported an autologous engineered skin substitute (ESS) for excised, full-thickness burns that provides permanent wound closure [6,11,12]. For this model of ESS, keratinocytes from the epidermis and fibroblasts from the dermis are isolated from a biopsy of a patient's remaining viable skin. The cells are then expanded in vitro until sufficient numbers are obtained and then inoculated into a collagen-glycosaminoglycan scaffold (CGS). After inoculation, the ESS is incubated in vitro for one to two weeks to allow the formation of an epidermal-dermal construct that may be grafted onto the patient. Over time, the ESS graft remodels, becomes soft and pliable, and restores the essential physiologic barrier to fluid loss and infection.

Despite the success of this model, much remains to be learned regarding the relationships between the degradation of the collagen scaffold and synthesis of extracellular matrix during the remodeling process and how these factors integrate across scales ranging from nanometers to centimeters to generate the mechanical and physiologic properties of the engineered skin. To evaluate these properties, the ESS containing human cells were tested mechanically at two weeks of incubation in vitro and at six weeks after grafting to a full-thickness wound in athymic mice. Additional context for changes in the remodeling and mechanical properties of the ESS was obtained by comparing ESS in vitro to an acellular CGS, or to a dermal skin substitute (DSS) consisting of CGS populated with hF and by comparing grafted ESS to murine autograft or uninjured murine skin.

Materials and Methods

Cell Culture. Epidermal keratinocytes and dermal fibroblasts were coisolated from surgical discard (neonatal foreskins)

[1]Corresponding author.
Contributed by the Bioengineering Division of ASME for publication in the JOURNAL OF BIOMECHANICAL ENGINEERING. Manuscript received October 15, 2013; final manuscript received December 12, 2013; accepted manuscript posted December 19, 2013; published online April 10, 2014. Assoc. Editor: David Corr.

obtained under a protocol approved by the University of Cincinnati Institutional Review Board. The cells were incubated and subcultured with selective growth media [13–15] and cryopreserved at low passage numbers. For this study, passage three human dermal fibroblasts (hF) were thawed and incubated in T-150 tissue culture flasks containing supplemented Dulbecco's modified Eagle's medium [15]. Human keratinocytes (hK) were propagated in modified medium MCDB153 [16,17].

ESS Fabrication and Incubation. Collagen-glycosaminoglycan scaffolds (CGS) were fabricated from bovine skin collagen and chondroitin-6-sulfate as described elsewhere [15,18]. Briefly, bovine skin collagen was solubilized in 0.5M acetic acid, coprecipitated with chondroitin-6-sulfate, and homogenized. The homogenate was injected into casting frames, frozen, lyophilized, crosslinked via thermal dehydration in a vacuum oven at 140 °C for 24 h, and sterilized by γ-irradiation.

Six γ-irradiated CGS, measuring approximately 9 cm $\times$ 9 cm, were rehydrated with 70% isopropanol and rinsed repeatedly with medium UCMC160. DSS were prepared by inoculation of hF onto CGS at a density of 0.5×10^6 cells/cm^2. On the following day (defined as day 0), five ESS were prepared by inoculation of hK onto five of the six DSS at a density of 1.0×10^6 cells/cm^2. DSS and ESS were maintained at the air-liquid interface by placing them upon a perforated stainless steel frame, a cotton filter paper, and a nonadherent, polypropylene dressing (N-terface®, Winfield Laboratories, Richardson, TX). The cotton filter paper acted as a wick for medium transport between the dermal component of the ESS and the medium in the culture dish. The N-terface dressing facilitated ESS transfer between tissue culture dishes. ESSs were incubated at 37 °C and 5% CO_2 with daily medium changes until they were either grafted to animals (day 14) or tested mechanically (day 15).

Surface Electrical Capacitance. Surface electrical capacitance (SEC) provides a surrogate measurement of the formation of the epidermal barrier as a function of surface hydration. SEC measurements of ESS surface hydration decrease as the barrier is established. SEC measurements were made with a NOVA dermal phase meter (DPM 9003, NOVA Technology, Portsmouth, NH). Four SEC measurements were made on each DSS ($n = 1$) and ESS ($n = 5$) on days 7 and 13. SEC measurements are presented in DPM units as mean ± SEM.

Animal Surgery. Animal care and use protocols were approved by the University of Cincinnati Institutional Animal Care and Use Committee. On incubation day 14, two ESS were each cut into four 2 cm $\times$ 2 cm grafts ($n = 8$). The grafts were applied to full thickness excisional wounds on the right flanks of eight athymic (homozygous nu/nu) mice, sutured, and dressed [15,19]. Eight additional mice were prepared with autograft, where the excised skin was removed intact, rotated 180 deg, and sutured onto the same site. Animals were sacrificed after six weeks, and the entire circumference between the fore and hind limbs was excised after orientation landmarks were made with an indelible marker.

Uniaxial Tensile Testing. Mechanical tests were conducted on CGS (rehydrated as above), DSS, ESS, grafted ESS, autografts, and native mouse skin. Prior to mechanical testing, samples were maintained on cotton filter paper moistened with culture medium and incubated at 37 °C and 5% CO_2. This culture condition maintained a moist dermal surface and a dry epidermal environment. Dumbbell-shaped samples (26 mm in total length with a gauge region 6 mm long and 2 mm wide) were prepared with a stainless-steel punch. The punch geometry was designed in consideration of minimizing the grip effects and the inherent constraints of the size of the animal grafts. CGS, DSS, and ESS samples did not possess any discernible preferred orientation and were punched out to maximize the number of samples available for testing ($n > 6$). Grafted ESS, autograft, and mouse skin samples were punched from the excised skin so that the long axis of the dumbbell shape followed the rostral-caudal axis of the animal. If possible, two samples were punched from each grafted ESS and autograft to provide a duplicate if needed (see below). A single mouse skin sample was also excised and punched with the same orientation from the contralateral flank of each mouse.

Mechanical testing was conducted at room temperature and in ambient conditions (Fig. 1(*a*)). The tab regions of the sample (8 mm wide $\times$ 10 mm long) were covered with gauze and clamped with rubber-faced compression grips that were connected to a materials testing system (100 R; TestResources Inc., Shakoppe, MN). Mounted samples were stretched to a preload of 0.01 N at a rate of 0.04 mm/s, preconditioned using a sinusoidal profile consisting of 10 cycles at 0.2 cycles/s and an amplitude of 1.5 mm of displacement, and finally loaded to failure at 1.2 mm/s (~10%/s). Load, time, and grip position data were collected at a sampling rate of 48 Hz and exported as comma separated values (CSV) files for analysis.

Samples that failed outside of the gauge region were disqualified from data collection. For those cases where two grafted ESS or autograft samples were obtained from the same graft and the mechanical tests were both valid, the average of the mechanical data collected from the two samples was taken as the value for that graft. Three of the eight grafted ESS samples were also disqualified because the graft area had contracted to the extent that the ESS portion of the sample could not be secured between the grips.

Histology. Sample thickness (reported as mean ± SEM) was assessed by averaging five measurements made from digital images of histological sections obtained from the remaining sample material immediately adjacent to the punched out gauge region of each sample. Histology samples were also collected at incubation day 14 prior to grafting for direct comparison with the grafts after six weeks of remodeling. Samples were fixed in 10% formalin and embedded in paraffin. Four micrometer thick sections were stained with Tango (Anatech LTD, Battle Creek, MI), a replacement dye for hematoxylin.

Human Leukocyte Antigen. Persistence of human ESS on murine hosts was confirmed by staining paraffin embedded sections of grafted ESS. Following antigen retrieval in 10 mM sodium citrate at *p*H 6 and 90 °C, a common epitope on human leukocyte antigens (HLA) A, B, and C (ab70328, Abcam, Cambridge, MA) was detected with a mouse-on-mouse fluorescein-labeled antibody kit (FMK-2201, Vector Laboratories, Inc., Burlingame, CA) following manufacturers protocols.

Data Analysis. Mechanical data were imported into Matlab R2010b (Mathworks Inc., Natick, MA) and analyzed with custom code to calculate the structural properties of linear stiffness (N/mm), ultimate tensile load (UTL) at failure (N), maximum extension at failure (mm), and the energy absorbed up to the point of failure (N-mm) (Fig. 1(*b*)). The force data were smoothed with a five-point moving average filter, after which the instantaneous stiffness was determined from the first derivative of the force-displacement curve by using a centered finite difference approximation given by

$$S_i = (F_{i+1} - F_{i-1})/(x_{i+1} - x_{i-1}) \quad (1)$$

where S_i is the instantaneous stiffness at time point i, and F and x are the load-cell force and grip-position of the preceding (x-i) and following ($x + i$) data points, respectively [20]. Linear stiffness was then determined from the slope of the best-fit line of the raw data over a range of 1 mm of displacement that also included the highest instantaneous stiffness [21]. Ultimate load at failure was defined as the highest load achieved during the test, and maximum

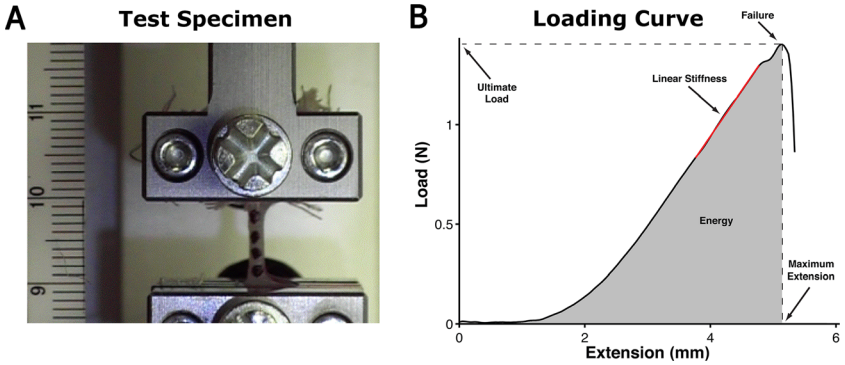

Fig. 1 Representative test specimen and loading curve. (*a*) A dog-bone-shaped sample placed between grips and gauze for uniaxial failure testing. Markers were placed on the surface to facilitate strain analysis if needed (scale = mm). (*b*) The load-extension curve of an ESS graft depicting where the structural properties of an ESS graft were extracted from, including the ultimate load at failure (N), the maximum extension at failure (mm), the linear stiffness (N/mm) (red-line), and the energy absorbed up to failure (N-mm) (gray area under the curve).

extension at failure was defined as the coincident sample extension at that point. The energy absorbed by the sample was defined as the area under the load-extension curve up to the point of maximum failure and calculated using numerical integration. Mechanical properties are reported as mean ± SEM.

Statistical Analysis. The data were subjected to nonparametric statistical analysis by the Kruskal–Wallis test for overall differences in the structural parameters (linear stiffness, ultimate tensile load, maximum extension, and energy absorbed before failure). Pairwise comparisons with the Wilcoxon rank sum test were then done to determine significant differences between groups ($p < 0.05$). The data for each of the six groups are presented in box and whisker plots that show the median, interquartile range, and maximum and minimum values. All analyses were conducted using SAS, version 9.3 (SAS Institute Inc., Cary, NC).

Results

Remodeling. Construct remodeling was assessed primarily from histological sections (Fig. 2) and from other gross measurements and observations as described below. CGS were porous and variable in thickness (335 ± 97 μm). The addition of fibroblasts to CGS resulted in rapid reduction in sponge surface area by 20% ± 6% within the first 24 h of culture. After two weeks the surface area of the DSS continued to decrease to 33.6% of the initial area. DSS thickness increased (406 ± 37 μm) compared to CGS and the fibroblasts remained localized to the top half of the scaffold. The addition of keratinocytes to form an ESS resulted in a greater reduction in surface area (52% ± 4%) and an increase in thickness (595 ± 27 μm). SEC measurements on ESS at 7 and 13 days (755 ± 7 DPM and 10 ± 6 DPM, respectively) indicated that an epidermal barrier had begun to form. By comparison, SEC measurements on DSS did not change between days 7 and 13 (843 ± 2 DPM and 855 ± 8 DPM, respectively). Photomicrographs at day 14 (Fig. 2) confirmed that an epidermal-dermal anatomy had formed. These images show a cornified layer that was separated from a fibroblast remodeled dermal component by a stratified and nucleated epithelium.

Grafted ESS continued to mature during the six weeks after grafting. Both grafted ESS and autograft margins remained visible (dotted white lines) on the mice at two weeks post-surgery (Fig. 3). At six weeks postsurgery, ESS boundaries were still observable. In contrast, autograft boundaries were more difficult to identify. In addition, the scaffold was still visible in histological sections of grafted ESS, and HLA staining confirmed that the ESS was populated with human cells (not shown). Measured thicknesses for grafted ESS (763 ± 80 μm) and autograft (761 ± 74 μm) were comparable and greater than intact murine skin (572 ± 34 μm).

Mechanical Properties

In vitro *Samples*. Responses to loading prior to failure revealed significant differences in the constructs as a function of cellular populations and transplantation (Fig. 4). The baseline linear stiffness of a hydrated acellular collagen scaffold (CGS) was 0.023 ± 0.004 N/mm. Linear stiffness increased significantly when fibroblasts (DSS) and fibroblasts and keratinocytes (ESS) were added and allowed to populate and remodel the matrix for two weeks in vitro (Fig. 5). Although more force was required to deform an ESS than a DSS for a given distance, average DSS stiffness was numerically greater but not statistically different (0.072 ± 0.021 N/mm) than average ESS stiffness (0.060 ± 0.012 N/mm) due to a sharp nonlinear increase in the DSS loading curve just before reaching UTL. UTL, energy, and maximum extension also increased with the addition of cells with the ESS achieving the highest values among in vitro constructs (Fig. 5).

In vivo *Samples*. Significant differences in all four of the structural mechanical properties tested were observed between ESS and grafted ESS at six weeks after grafting (Fig. 5). Linear stiffness, UTL, and energy of grafted ESS increased more than sevenfold (0.467 ± 0.108 N/mm), fourfold (1.50 ± 0.54 N), and nearly twofold (2.79 ± 1.49 N-mm), respectively, compared to ESS in vitro. Maximum extension at failure (5.65 ± 1.12 mm) decreased significantly compared to in vitro ESS (8.86 ± 1.52 mm). Grafted ESS were also significantly stiffer than native murine skin (0.221 ± 0.061 N/mm) but not compared to autograft (0.341 ± 0.115 N/mm). Conversely, maximum extension was significantly higher for murine skin (12.30 ± 1.15 mm) than in grafted ESS or autograft (8.85 ± 1.62). Although UTL was highest in grafted ESS and energy absorbed until failure was highest in murine skin, no significant differences in these properties were found among in vivo samples.

Discussion

Although ESS have provided an alternative for treating patients with massive burns and other conditions that require skin grafting, improvements are required to restore the complete anatomy and physiology of healthy, uninjured skin. Therefore, a comprehensive understanding of the remodeling process before and after transplantation is fundamental to restoring the repaired skin's organization and functional properties, such as tissue stability and range of

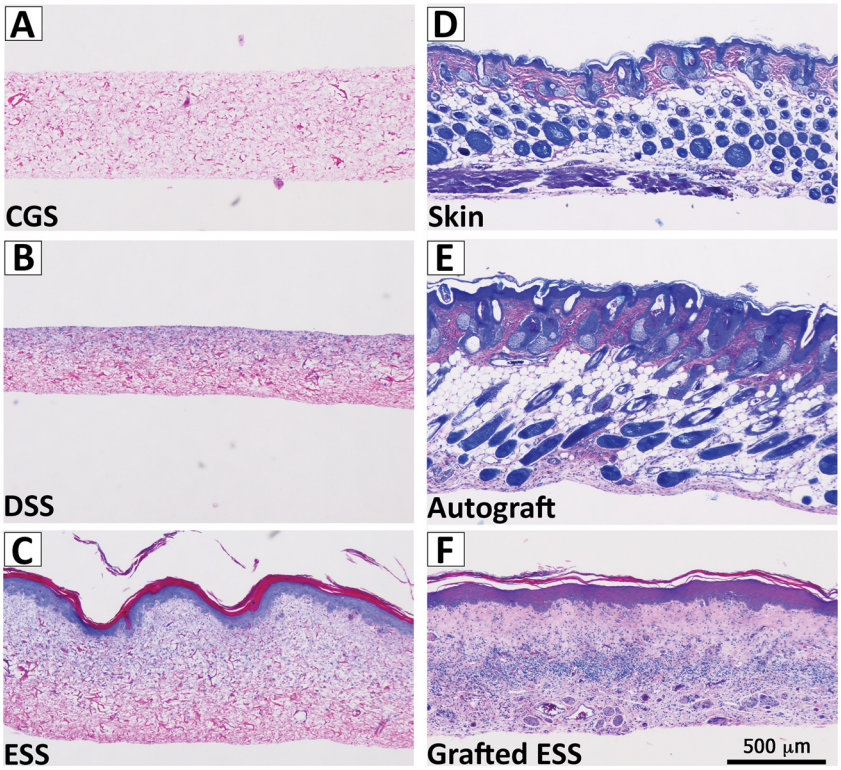

Fig. 2 Sample histology. Representative histological sections show the progression of engineered skin substitute (ESS) remodeling from (*a*) an acellular collagen-glycosaminoglycan sponge (CGS), (*b*) dermal skin substitute (DSS) cultured in vitro two weeks, (*c*) ESS cultured in vitro two weeks, (*d*) grafted ESS six weeks post implantation on athymic mice, and compared to (*e*) mouse autograft, and (*f*) native mouse skin. Scale bar = 0.5 mm.

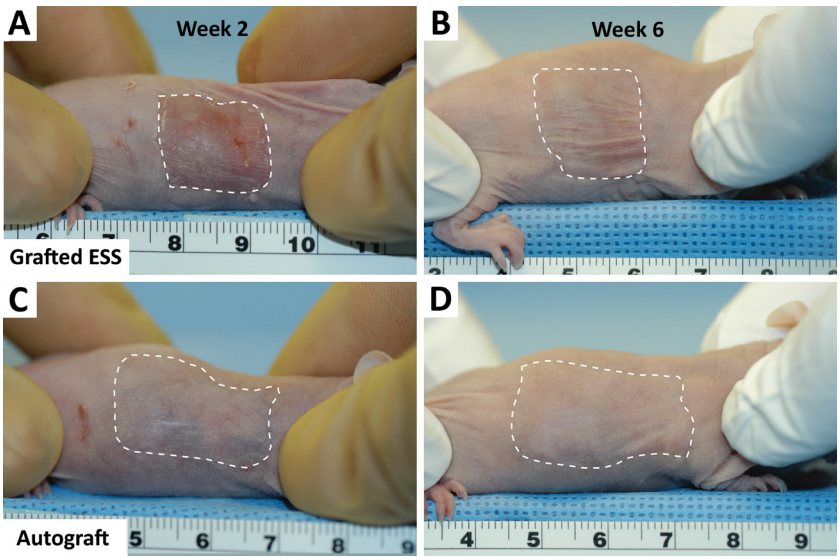

Fig. 3 Grafted ESS and autograft postsurgery. (*a*) At two weeks postsurgery the grafted ESS is still visible. (b) At six weeks postsurgery the grafted ESS margins are less distinguishable from the surrounding skin. The autograft shows better integration and a better appearance at (*c*) two weeks that (*d*) continues to improve so that at six weeks it is difficult to find the margins. Scale is in cm.

motion [22], that promote restoration of the activities of daily living and quality of life. In addition, improvement of the mechanical properties of ESS in vitro would facilitate surgical application, reduce graft loss due to mechanical shear, simplify nursing care, and allow for earlier mobilization of patients after grafting.

The mechanical properties of skin arise primarily from the composition and organization of ECM in the dermis, which varies with anatomic site, age, and genetic background of the individual [23]. This variability gives rise to a large range of reported mechanical properties of human skin, including ultimate tensile

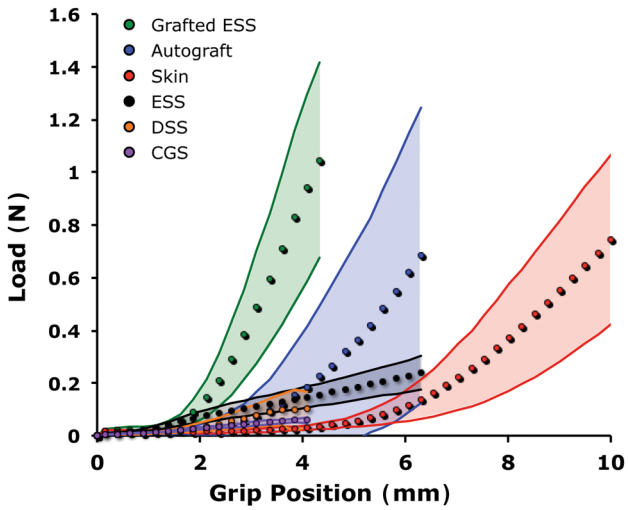

Fig. 4 Averaged load-displacement curves. The averaged sample responses (filled circles) are depicted prior to the point of failure of the first sample in the group. The corresponding standard deviation is indicated by the shaded region. The addition of fibroblasts (DSS) and coculture of fibroblasts and keratinocytes (ESS) increased the stiffness and UTL of the construct before failure occurred. Substantial improvements in mechanical properties developed in six-week grafted ESS. The grafted ESS and autograft were both stiffer and less compliant than the native mouse skin.

strength (UTS), which ranges from approximately 1 to 40 MPa [24,25]. The bulk tensile mechanical properties of skin derive primarily from the collagen fibers in the dermis [24]. When the tissue is stretched uniaxially it exhibits strain-stiffening behavior that is attributed to the progressive recruitment of collagen fibers that rotate, align, and straighten in the direction of stretch until the point of failure. Alterations in this characteristic J-shaped load-displacement curve reflect differences in the microstructure of the tissue, such as collagen fiber morphology, organization, cross-link density, and the presence or absence of other ECM proteins, such as elastic fibers and proteoglycans. For example, Oxlund et al. reported that controlled enzymatic digestion of elastic fibers in rat skin changed the shape of the loading curve [26]. Although the failure properties remained unchanged, the treated skin samples were more extensible and less stiff in the early portion of the curve (i.e., toe region) than controls, indicating that elastin fibers are important load-bearing elements for small deformations but not for tissue strength. Experiments such as these demonstrate that the biomechanical analysis of engineered skin can provide important insights on the microstructure and compositional changes that may occur during the remodeling process.

In this study, alterations in the mechanical behavior of ESS were observed for both the in vitro and in vivo phases of the remodeling process. Several factors were found to contribute to ESS mechanical strength including synthesis of new ECM and degradation of scaffold, cellular replication, differentiation, and tissue morphogenesis. The addition of fibroblasts to the CGS resulted in a substantial reduction in scaffold area and a modest increase in the mechanical properties (Figs. 4 and 5). These changes are similar to those observed in collagen gel systems where fibroblasts rapidly compact the gel, realign fibers, and generate endogenous tension over a few days [27–29].

The addition of keratinocytes in close proximity to the fibroblasts in the scaffold led to important morphological changes in the ESS that included the formation of the dermal-epidermal junction (DEJ) and a differentiated and stratified epidermis. Several of the components that make up these structures have been identified as important components of the biomechanical structure of the tissue, including involucrin, loricrin, and the keratin intermediate filaments bound together by desmosomes [30,31]. These components have been identified in ESS previously in this lab [14] and are likely responsible for part of the increase in mechanical properties observed here. Other studies have also demonstrated a strong correlation between ESS tensile strength and the properties of the engineered epidermis that improve with longer culture times [27,32]. Ebersole et al., using a similar culture system based on electrospun fibers instead of biopolymer sponges, reported an average UTS value of 0.4 MPa at 14 days that increased to 0.6 MPa at 21 days. The average UTS of ESS in this study, calculated by dividing UTL by the width of the gauge region and average sample thickness, was comparable and estimated to be 0.3 MPa. Progressive improvements in ESS mechanical properties with increased in vitro culture time are, however, limited. Previous work in this laboratory has shown that after approximately four weeks, the ESS loses mechanical stability (unpublished data), which suggests that the fibroblasts are unable to produce a well-connected network of ECM fast enough to replace the degraded and weakened scaffold. As a result, ESS must be grafted to host tissue within approximately two to three weeks for continued development.

The in vivo environment provides a complex, multifactorial environment that significantly stiffened and strengthened the grafted ESS. Although some of the processes responsible for these changes were likely maintained or initiated under in vitro conditions, the in vivo environment undoubtedly supported formation of a stable dermal ECM composed of collagen, and likely complexed to the DEJ. Access to a vascular supply, inflammatory mediators, growth factors, and an altered mechanical environment are all likely contributors to the changes in mechanical behavior and remodeling observed here. Stiffness and UTL increased approximately eightfold and fourfold, respectively, after ESS transplantation to wounds in athymic mice. An average UTL of 1.5 N corresponds to an estimated UTS of 1.0 MPa, which is within the range of reported values for human skin, albeit at the extreme lower boundary [24,25,33]. These results are consistent with the outcomes in clinical studies [9] in which burn patients are able to begin ambulation within one month after grafting without mechanical failure of the healing ESS.

With respect to ECM, although the amount of collagen in the grafted ESS was not quantified, it is reasonable to expect that the increase in grafted ESS stiffness and strength reflected higher amounts of collagen. Grafted ESS, however, also failed at lower maximum extension than any other group including the in vitro ESS. The shorter toe region in these samples (Fig. 4) suggests that there are few elastic fibers (if any) present at the time point tested. Elastic fibers are recruited at the onset of stretch and shift the onset of strain-stiffening behavior to higher levels of tissue stretch. The fact that maximum extension at failure is higher in vitro likely reflects the compliance of the epidermal layer and that not enough collagen has been produced in vitro for the dermal component to provide full mechanical support. Elastic fiber production has been observed in ESS grafted to nude mice by others [34]. Berthod et al. detected isolated aggregates of human elastin five days after transplantation that became more homogenously deposited after 40 days, but the elastic fiber network did not begin to become well organized and structured until 90 days after transplantation [34]. Because the grafts in this study were only allowed to remodel for 42 days, it is likely that sufficient time had not elapsed for the human cells populating the graft to produce a mature elastic network.

The mechanical response of murine autograft and intact skin were also assessed as controls so that contributions to the remodeling process from the surgery could be evaluated. Murine autograft was significantly less compliant and stiffer than intact skin, demonstrating that some of the changes in mechanical properties observed in grafted ESS can be attributed to inflammation and the wound healing process. These controls, however, do not provide the reference points for comparison that native human skin before

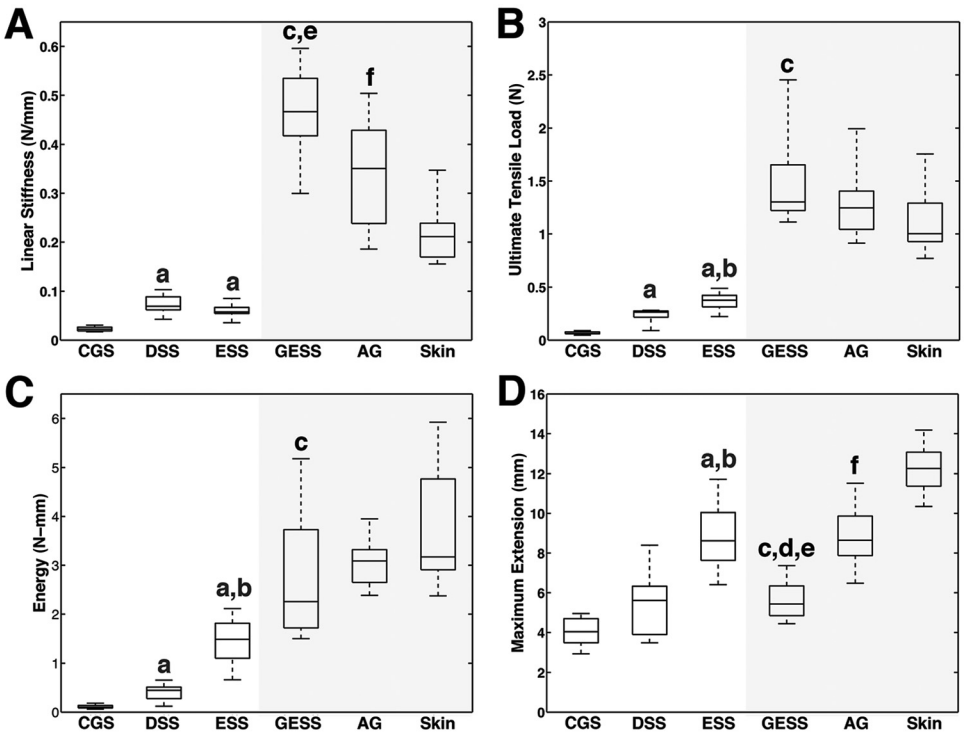

Fig. 5 Structural property boxplots. (a) Linear stiffness, (*b*) ultimate tensile load, (*c*) energy, (*d*) maximum extension for CGS ($n = 11$), DSS ($n = 6$), ESS ($n = 23$), grafted ESS (GESS, $n = 5$), autograft (AG, $n = 8$), and intact murine skin ($n = 13$). Shaded area corresponds to in vivo samples collected from athymic mice at six weeks after grafting. a indicates significant difference ($p < 0.05$) between in vitro group with CGS, b indicates significant difference ($p < 0.05$) between ESS and DSS. c indicates significant difference ($p < 0.05$) between grafted ESS and ESS. d indicates significant difference ($p < 0.05$) between grafted ESS and autograft. e indicates significant difference ($p < 0.05$) between grafted ESS and ungrafted murine skin. f indicates significant difference ($p < 0.05$) between autograft and skin.

and after grafting could provide; human skin is substantially thicker, stiffer, and stronger than mouse skin. Thus, the comparison with murine skin is limited in its comparative value to human skin, and simply means that grafted ESS gains at least as much mechanical strength as uninjured mammalian skin, although not human. Therefore, future studies should be performed with split-thickness human skin as a control [19,35].

Although some relationships between ECM microstructure and tissue function have been clearly established, a more detailed view of how the constituents of the ECM are organized locally and integrated globally across scales to produce the tissue's mechanical properties (i.e., multiscale mechanical interactions) is necessary. Small local changes in the ECM can have a profound effect on the mechanical function of the tissue, a phenomenon that is observable in a number of genetic connective tissue disorders [36,37], and that partially explains the variability in skin mechanical properties. With regard to ESS, because the relationships between microscopic structure and macroscopic function are only understood at an elementary level, it is difficult to evaluate where improvements need to be made in these constructs. With many complicated phenomena operating at multiple scales and regulated to varying degrees by the properties of the ECM, mechanical models become a necessary tool for the elucidation of the relationships between individual ECM components and the aggregate properties and function of tissues [38,39]. Such computational models, when coupled with in vivo and in vitro data, could be used to understand and assess how the microstructure in an ESS produces its mechanical properties so that new models of improved ESS can be designed. The data obtained in this study serve as a basis for the development of such models. Model construction, in turn, fosters the development of fresh ideas for examining ESS remodeling and for designing new studies to obtain model data. Such studies may include measurements of the spatial and temporal distributions of collagen and elastin via biochemical assays [40] and multiphoton microscopy [41] and analysis of gene expression via microarray analysis [8].

Conclusions

The data reported from this study show the dynamic capabilities of engineered skin to change over time, to respond to the systemic physiology after transplantation, and to increase in mechanical strength. From this study, it may be concluded that the development of mechanical properties in engineered skin depends on the combination of specific cellular populations (number and type), biopolymer scaffolds, and time. Furthermore, the conditions for fabrication and maturation of ESS in vitro are deficient and do not promote stable long-term tissue morphogenesis. Transplantation of engineered skin to wounds provides a complete complement of factors required to restore the essential mechanical and biological properties for stable and durable tissue repair, but it does not represent true regeneration. Morphogenesis and remodeling of ESS requires more time than native skin autograft after transplantation to excised, full-thickness wounds but reaches comparable mechanical strength. Future studies of mechanical properties of ESS before and after transplantation are expected to allow identification and regulation of factors that are required for reductions of morbidity in treatment of burns, scars, and chronic wounds.

Acknowledgment

The authors would like to acknowledge Nat Dyment and David Butler for assistance with mechanical testing, Dorothy Supp and

Rachel Zimmerman with the mouse surgeries, Laura James with statistical analysis of the data, and Chris Lloyd and Jill Pruska with ESS fabrication and cell culture. Funding for this project was provided by NIH grants GM079542 and AR063967 and the State of Ohio Third Frontier Clinical Tissue Engineering Center.

References

[1] Supp, D. M., and Boyce, S. T., 2005, "Engineered Skin Substitutes: Practices and Potentials," Clin. Dermatol., **23**(4), pp. 403–412.

[2] Boyce, S. T., 2004, "Fabrication, Quality Assurance, and Assessment of Cultured Skin Substitutes for Treatment of Skin Wounds," Biochem. Eng. J., **20**(2), pp. 107–112, 2004.

[3] American Burn Association, 2013 National Burn Repository, American Burn Association, Chicago, IL.

[4] MacNeil, S., 2007, "Progress and Opportunities for Tissue-Engineered Skin," Nature, **445**(7130), pp. 874–880, 2007.

[5] Zeng, Q., Macri, L. K., Prasad, A., Clark, R. A. F., Zeugolis, D. I., Hanley, C., Garcia, Y., and Pandit, A., 2011, "Skin Tissue Engineering", Comprehensive Biomaterials, P. Ducheyne, K. Healy, D. E. Hutmacher, D. W. Grainger, and C. J. Kirkpatrick, eds., Elsevier, Philadelphia, PA, pp. 467–499.

[6] Boyce, S. T., Kagan, R. J., Greenhalgh, D. G., Warner, P., Yakuboff, K. P., Palmieri, T., and Warden, G. D., 2006, "Cultured Skin Substitutes Reduce Requirements for Harvesting of Skin Autograft for Closure of Excised Full-Thickness Burns," J. Trauma, **60**(4), pp. 821–829.

[7] Brusselaers, N., Pirayesh, A., Hoeksema, H., Richters, C. D., Verbelen, J., Beele, H., Stijn, I. B., and Monstrey, S., 2010, "Skin Replacement in Burn Wounds," J. Trauma, 68(2), pp.490–501.

[8] Powell, H. M., McFarland, K. L., Butler, D. L., Supp, D. M., and Boyce, S. T., 2009, "Uniaxial Strain Regulates Morphogenesis, Gene Expression, and Tissue Strength in Engineered Skin, Tissue Eng. A., **16**(3), pp. 1083–1092.

[9] Boyce, S. T., Supp, A. P., Wickett, R. R., Hoath, S. B., and Warden, G. D., 2000, "Assessment With the Dermal Torque Meter of Skin Pliability After Treatment of Burns With Cultured Skin Substitutes," J. Burn Care Res., **21**(1), pp. 55–63.

[10] Grenier, G., Remy-Zolghadri, M., Larouche, D., Gauvin, R., Baker, K., Bergeron, F., Dupuis, D., Langelier, E., Rancourt, D., Auger, F. A., and Germain, L., 2005, "Tissue Reorganization in Response to Mechanical Load Increases Functionality," TIssue Eng., **11**(1–2), pp.90–100.

[11] Boyce, S. T., Kagan, R. J., Yakuboff, K. P., Meyer, N. A., Rieman, M. T., Greenhalgh, D. G., and Warden, G. D., "Cultured Skin Substitutes Reduce Donor Skin Harvesting for Closure of Excised, Full Thickness Burns," Ann. Surg., **235**(2), pp. 269–279.

[12] Boyce, S. T., Kagan, R. J., Meyer, N. A., Yakuboff, K. P., and Warden, G. D., 1999, "The 1999 Clinical Research Award. Cultured Skin Substitutes Combined With Integra Artificial Skin to Replace native Skin Autograft and Allograft for the Closure of Excised Full-Thickness Burns," J. Burn Care Rehabil., **20**(6), pp. 453–461.

[13] Swope, V. B., Supp, A. P., and Boyce, S. T., 2002, "Regulation of Cutaneous Pigmentation by Titration of Human Melanocytes in Cultured Skin Substitutes Grafted to Athymic Mice," Wound Rep. Regen., **10**(6), pp. 378–386.

[14] Boyce, S. T., Supp, A. P., Swope, V. B., Warden, G. D., 2002, Vitamin C Regulates Keratinocyte Viability, Epidermal Barrier, and Basement Membrane In Vitro, and Reduces Wound Contraction After Grafting of Cultured Skin Substitutes," J. Invest. Dermatol., **118**(4), pp. 565–572.

[15] Boyce, S. T., 1999, "Methods for the Serum-Free Culture of Keratinocytes and Transplantation of Collagen-GAG-Based Skin Substitutes," *Tissue Engineering Methods and Protocols Totowa*, J. Morgan and M. Yarmush, eds., Humana Press Inc., New Jersey, pp. 365–389.

[16] Boyce, S. T., and Ham, R. G., 1983, "Calcium-Regulated Differentiation of Normal Human Epidermal Keratinocytes in Chemically Defined Clonal Culture and Serum-Free Serial Culture," J. Invest. Dermatol., **81**, pp. 33s–40s.

[17] Shipley, G. D., and Pittelkow, M. R., 1987, "Control of Growth and Differentiation In Vitro of Human Keratinocytes Cultured in Serum-Free Medium," Arch. Dermatol., **123**(11), pp. 1541a–1544a.

[18] Boyce, S. T., Christianson, D. J., Hansbrough, J. F., 1988, "Structure of a Collagen-GAG Dermal Skin Substitute Optimized for Cultured Human Epidermal Keratinocytes," J. Biomed. Mater. Res., **22**(10), pp. 939–957.

[19] Boyce, S. T., Foreman, T. J., English, K. B., Stayner, N., Cooper, M. L., Sakabu, S., and Hansbrough, J. F., 1991, "Skin Wound Closure in Athymic Mice with Cultured Human Cells, Biopolymers, and Growth Factors," Surgery, **110**(5), pp. 866–876.

[20] Quinn, K. P., and Winkelstein, B. A., 2007, "Cervical Facet Capsular Ligament Yield Defines the Threshold for Injury and Persistent Joint-Mediated Neck Pain," J. Biomech., **40**(10), pp. 2299–2306.

[21] Alperin, M., Debes, K., Abramowitch, S., Meyn, L., and Moalli, P. A., 2008, "LOXL1 Deficiency Negatively Impacts the Biomechanical Properties of the Mouse Vagina and Supportive Tissues," Int. Urogynecol. J., **19**(7), pp. 977–986.

[22] Gibran, N. S., Wiechman, S., Meyer, W., Edelman, L., Fauerbach, J., Gibbons, L., Holavanahalli, R., Hunt, C., Keller, K., Kirk, E., Laird, J., Lewis, G., Moses, S., Sproul, J., Wilkinson, G., Wolf, S., Young, A., Yovino, S., Mosier, M. J., Cancio, L. C., Amani, H., Blayney, C., Cullinane, J., Haith, L., Jeng, J. C., Kardos, P., Kramer, G., Lawless, M. B., Serio-Melvin, M. L., Miller, S., Moran, K., Novakovic, R., Potenza, B., Rinewalt, A., Schultz, J., Smith, H., Dylewski, M., Wibbenmeyer, L., Bessey, P. Q., Carter, J., Gamelli, R., Goodwin, C., Graves, T., Hollowed, K., Holmes, J. 4th, Noordenbas, J., Nordlund, M., Savetamal, A., Simpson, P., Traber, D., Traber, L., Nedelec, B., Donelan, M., Baryza, M. J., Bhavsar, D., Blome-Eberwein S., Carrougher, G. J., Hickerson, W., Joe, V., Jordan, M., Kowalske, K., Murray, D., Murray, V. K., Parry, I., Peck, M., Reilly, D., Schneider, J. C., Ware, L., Singer, A. J., Boyce, S. T., Ahrenholz, D. H., Chang, P., Clark, R. A., Fey, R., Fidler, P., Garner, W., Greenhalgh, D., Honari, S., Jones, L., Kagan, R., Kirby, J., Leggett, J., Meyer, N., Reigart, C., Richey, K., Rosenberg, L., Weber, J., Wiggins, B., 2013, "American Burn Association Consensus Statements," J. Burn Care Res., **34**(4), pp. 361–385.

[23] Cua, A., Wilhelm, K. P., and Maibach, H., 1990, "Elastic Properties of Human Skin: Relation to Age, Sex, and Anatomical Region," Arch. Dermatol. Res., **282**(5), pp. 283–288.

[24] Lanir, Y., 1987, "Skin Mechanics," Handbook of Bioengineering, R. Skalak and S. Chien, eds., McGraw-Hill, Dallas, TX, pp. 11–25.

[25] Ní Annaidh, A., Bruyère, K., Destrade, M., Gilchrist, M. D., and Otténio, M., 2012, "Characterization of the Anisotropic Mechanical Properties of Excised Human Skin," J. Mech. Behav. Biomed. Mater., **5**(1), pp. 139–148.

[26] Oxlund, H., Manschot, J., and Viidik, A., 1988, "The Role of Elastin in the Mechanical Properties of Skin," J. Biomech., **21**(3), pp. 213–218.

[27] Lafrance, H., Yahia, L., Germain, L., Guillot, M., and Auger, F. A., 1995, "Study of the Tensile Properties of Living Skin Equivalents," Biomed. Mater. Eng., **5**(4), pp. 195–208.

[28] Sander, E. A. and Barocas, V. H., 2008, "Biomimetic Collagen Tissues: Collagenous Tissue Engineering and Other Applications," Collagen Structure and Mechanics, P. Fratzl, ed., Springer, New York, NY, pp. 475–504.

[29] Grinnell, F., and Petroll, W. M., 2010, "Cell Motility and Mechanics in Three-Dimensional Collagen Matrices," Ann. Rev. Cell Dev. Biol., **26**, pp. 335–361.

[30] Candi, E., Schmidt, R., and Melino, G., 2005, "The Cornified Envelope: A Model of Cell Death in the Skin," Nature Rev. Molec. Cell Biol., **6**(4), pp. 328–340.

[31] Fuchs, E., and Cleveland, D. W., 1998, "A Structural Scaffolding of Intermediate Filaments in Health and Disease," Science, **279**(5350), pp. 514–519.

[32] Ebersole, G., Anderson, P., and Powell, H., 2010, "Epidermal Differentiation Governs Engineered Skin Biomechanics," J. Biomech., **43**(16), pp. 3183–3190.

[33] Jansen, L., and Rottier, P., 1958, "Some Mechanical Properties of Human Abdominal Skin Measured on Excised Strips," Dermatol., **117**(2), pp. 65–83.

[34] Berthod, F., Germain, L., Li, H., Xu, W., Damour, O., and Auger, F. A., 2001, "Collagen Fibril Network and Elastic System Remodeling in a Reconstructed Skin Transplanted on Nude Mice," Matrix Biol., **20**(7), pp. 463–473.

[35] Robb, E. C., Bechmann, N., Plessinger, R. T., Boyce, S. T., Warden, G. D., and Kagan, R. J., "Storage Media and Temperature Maintain Normal Anatomy of Cadaveric Human Skin for Transplantation to Full-Thickness Skin Wounds," J. Burn Care Res., **22**(6), pp. 393–396.

[36] Holbrook, K. A., and Byers, P. H., 1989, "Skin Is a Window on Heritable Disorders of Connective Tissue," Am. J. Med. Genet., **34**(1), pp. 105–121.

[37] Bateman, J. F., Boot-Handford, R. P., and Lamandé, S. R., 2009, "Genetic Diseases of Connective Tissues: Cellular and Extracellular Effects of ECM Mutations," Nature Rev. Genetics, **10**(3), pp. 173–183.

[38] Sander, E. A., Stylianopoulos, T., Tranquillo, R. T., and Barocas, V. H., 2009, "Image-Based Multiscale Modeling Predicts Tissue–Level and Network-Level Fiber Reorganization in Stretched Cell-Compacted Collagen Gels," Proc. Nat. Acad. Sci. USA, **106**(42), pp. 17675–17680.

[39] Hadi, M. F., Sander, E. A., and Barocas, V. H., 2012, "Multiscale Model Predicts Tissue-Level Failure From Collagen Fiber-Level Damage," ASME J. Biomech. Eng., **134**(9), pp. 091005.

[40] Sander, E. A., Barocas, V. H., and Tranquillo, R. T., 2011, "Initial Fiber Alignment Pattern Alters Extracellular Matrix Synthesis in Fibroblast-Populated Fibrin Gel Cruciforms and Correlates With Predicted Tension," Ann. Biomed. Eng., 2011, pp. 1–16.

[41] Cicchi, R., Kapsokalyvas, D., De Giorgi, V., Maio, V., Van Wiechen, A., Massi, D., Lotti, T., and Pavone, F. S., 2010, "Scoring of Collagen Organization in Healthy and Diseased Human Dermis by Multiphoton Microscopy," J. Biophotonics, **3**(1–2), pp. 34–43.